Mapping the magnetic phase diagram of metastable fct Fe/Cu(100) using Co atoms

J. P. Pierce,[1,2] M. A. Torija,[1,2] J. Shen,[1,*] and E. W. Plummer[1,2]
[1]*Solid State Division, Oak Ridge National Laboratory, Oak Ridge, Tennessee 37831*
[2]*Department of Physics, The University of Tennessee, Knoxville, Tennessee 37996*
(Received 23 April 2001; revised manuscript received 19 July 2001; published 20 November 2001)

In ultrathin Fe films grown at room temperature on Cu(100), observed thickness and temperature-dependent spin reorientations are preceded by structural transformations. We use a method involving Co capping atoms to generate a magnetic phase diagram for this system in the absence of these structural changes. The phase diagram shows that the recently observed stripe-phase melting in the Fe/Cu(100) system is related to the onset of a spin reorientation, rather than to a ferromagnetic-to-paramagnetic transition. In addition, the phase diagram allows us to determine the temperature-dependent anisotropy constants for Fe/Cu(100) films.

DOI: 10.1103/PhysRevB.64.224409 PACS number(s): 75.70.Ak, 75.30.Gw, 75.30.Kz

Recent work on perpendicularly magnetized Fe/Cu(100) ultrathin films has revealed interesting evolution in their magnetic-domain structure as the film thickness is varied at a fixed temperature.[1,2] Two-step disordering of a micrometer-sized stripe phase has been observed experimentally[1] in close agreement with theoretical predictions.[3] Theoretically, the melting of this stripe phase could result from the close proximity of the system temperature to either the critical temperature for a spin-reorientation transition (SRT), or the critical temperature for a ferromagnetic to paramagnetic phase transition (Curie temperature), depending on which one is lower. Such an issue can, in principle, be resolved by obtaining a magnetic phase diagram of the system.

A considerable number of efforts have been made to map out the magnetic phase diagram of the Fe/Cu(100) system.[4–6] The phase diagrams obtained so far, while extremely interesting, have shown magnetic phase transitions that are greatly affected by various types of structural transitions.[7–10] The aforementioned stripe phase melting, however, is likely to be a pure magnetic phase transition since it was observed in the thickness (<4 ML) and temperature regime (<310 K) in which the films are structurally uniform in a face-centered-tetragonal (fct) phase. A thorough understanding of such a phase transition, thus, requires a *pure* magnetic phase diagram obtained in the absence of these structural transitions.

Here, we employ a method involving magnetic capping atoms to obtain information about the magnetic phase diagram of the underlying Fe/Cu(100) films in the absence of structural transitions. It is known that magnetic capping atoms can modify the effective anisotropy of a system such that an SRT can take place when the number of capping atoms thickness reaches some critical value.[11] We have previously reported a method for using this phenomenon to determine the critical thickness of SRT for the uncapped Fe film.[12,13] Here, we use this technique to map a *pure* magnetic phase diagram that completely separates out the influence of structural transitions. The phase diagram indicates that the critical temperature for SRT of the Fe/Cu(100) system is lower than the Curie temperature, which implies that the melting of the stripe phase reflects the proximity of the system to the SRT temperature rather than the Curie temperature. Our data have also been used to determine the temperature-dependent anisotropy constants for the Fe/Cu(100) films.

Experiments were performed in an ultrahigh vacuum (UHV) system with a base pressure lower than 7×10^{-11} Torr. The system was equipped with facilities for low-energy electron diffraction (LEED), Auger electron spectroscopy (AES), and magneto-optic Kerr effect (MOKE) studies. It was possible to operate the MOKE setup in both polar and longitudinal geometries by rotating the magnet around the sample. The Cu substrate was prepared by cycles of sputtering with Ne ions and annealing to 900 K until clean AES spectra and sharp (1×1) LEED patterns were obtained. The Fe(Co) films were evaporated from an Fe(Co) wire heated by electron-beam bombardment. The rate of deposition was controlled in each case by flux monitors, which were mounted on each source and calibrated by AES. The accuracy of using AES to determine film thickness was calibrated with scanning tunneling microscopy in a separate UHV chamber.

The iron films that we studied were always less than 4 ML

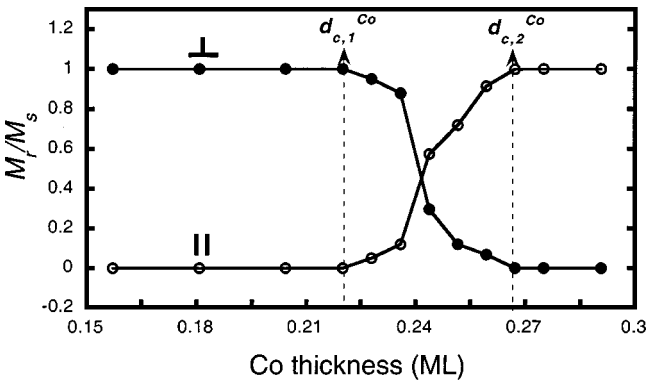

FIG. 1. Ratio of remanent magnetization ($\boldsymbol{M}_r$) to saturation magnetization ($\boldsymbol{M}_s$) of a Co capped 2.65-ML Fe/Cu(100) film measured with the magnetic field along the perpendicular (filled circles) and in-plane (open circles) directions as a function of Co capping layer thickness. The measuring temperature was 105 K. It is clear from the disappearance of the perpendicular signal and the appearance of the in-plane magnetization that the capping layer has induced a spin reorientation in the underlying Fe film.

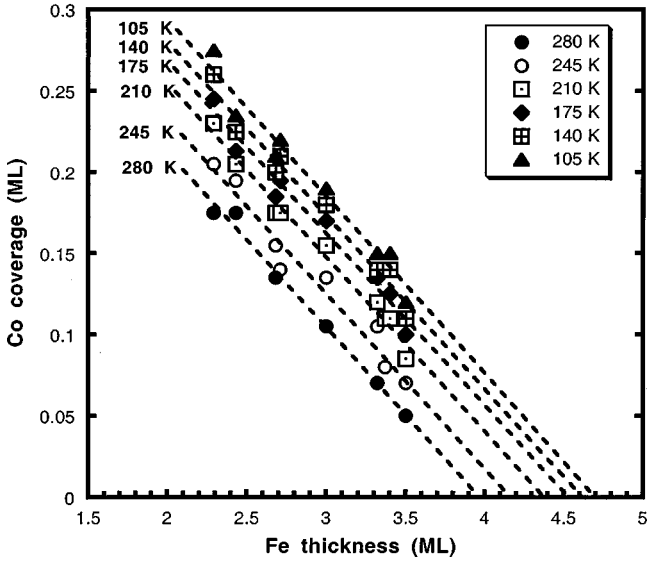

FIG. 2. Isothermal plots of the capping layer thickness required to start the spin reorientation as a function of base film thickness. Each set of data can be fit with a line that can be extrapolated to the horizontal axis that represents the absence of a capping layer. This gives the thickness at which a clean fct Fe film would begin to reorient at each temperature.

thick and were grown at room temperature (RT) to ensure that they were of the fct structure. After the growth of the Fe films, Co capping atoms were subsequently deposited onto the Fe film at 110 K. The capping atoms were added in steps as small as 0.005 ML and polar and longitudinal MOKE measurements were made after each deposition.

Figure 1 demonstrates a typical spin reorientation of a 2.65-ML Fe film induced by Co capping layers at 105 K. The ratios of remanent ($\boldsymbol{M}_r$) to saturation ($\boldsymbol{M}_s$) magnetization as determined from both polar (filled circles) and in-plane (open circles) MOKE hysteresis curves are displayed as a function of the amount of added cobalt. A perpendicular to in-plane SRT clearly starts to take place at about 0.22 ML of Co thickness, as evidenced by the decrease of perpendicular $\boldsymbol{M}_r$ and the increase of in-plane $\boldsymbol{M}_r$. When the Co thickness reaches 0.27 ML, the inplane $\boldsymbol{M}_r$ reaches saturation and the perpendicular $\boldsymbol{M}_r$ decreases to zero, indicating the completion of the SRT. We denote the starting point of the SRT (0.22 ML) as $d_{c,1}^{\mathrm{Co}}$, and the finishing point (0.27 ML) as $d_{c,2}^{\mathrm{Co}}$.

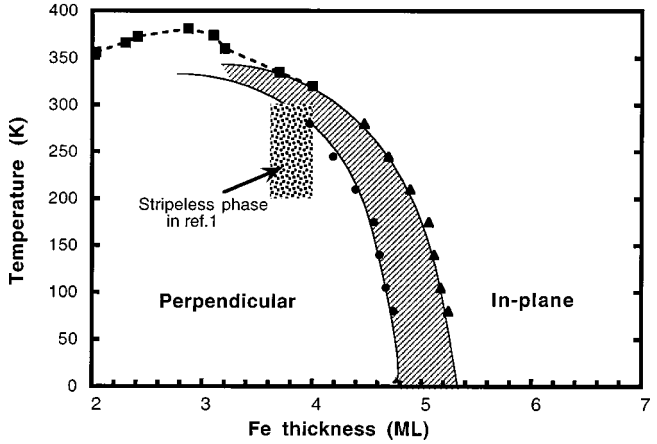

FIG. 3. Magnetic phase diagram for fct Fe on Cu(100). The shaded area is a transition regime in which the magnetization is either canted or made up of both perpendicular and in-plane domains. The gray horizontal bar marks the temperature regime in which a fct→fcc structural transition occurs.

Following this procedure, we have obtained values of both $d_{c,1}^{\mathrm{Co}}$ and $d_{c,2}^{\mathrm{Co}}$ for Fe films of various thickness at various temperatures. As mentioned, the Fe thickness was limited within the untransformed fct thickness regime (<4 ML), and the maximum temperature did not exceed room temperature in order to avoid any possible interdiffusion or structural change. In Fig. 2 we show the $d_{c,1}^{\mathrm{Co}}$ values as a function of thickness for Fe films obtained at various temperatures. Data points taken at each temperature clearly follow a linear fit, as indicated by the regression lines in the plot. The *x* axis intercept of each isotherm gives the value of the starting thickness ($d_{c,1}^{\mathrm{Fe}}$) at which an fct Fe/Cu(100) film would undergo a spin reorientation *without* Co *capping* at that particular temperature. For example, the easy axis of magnetization of a clean fct Fe/Cu(100) film at 210 K would begin to reorient from perpendicular to inplane at a thickness of 4.4 ML, if the previously mentioned fct→fcc structural transformation did not occur. The finishing point of the SRT of the Fe films ($d_{c,2}^{\mathrm{Fe}}$) has been determined in a similar way from a $d_{c,2}^{\mathrm{Co}}$ vs Fe thickness plot.

This data directly results in a magnetic phase diagram for fct Fe, as shown in Fig. 3. The shaded area represents the transition regime over which the easy axis of the film reorients from the surface normal to the in-plane direction. The

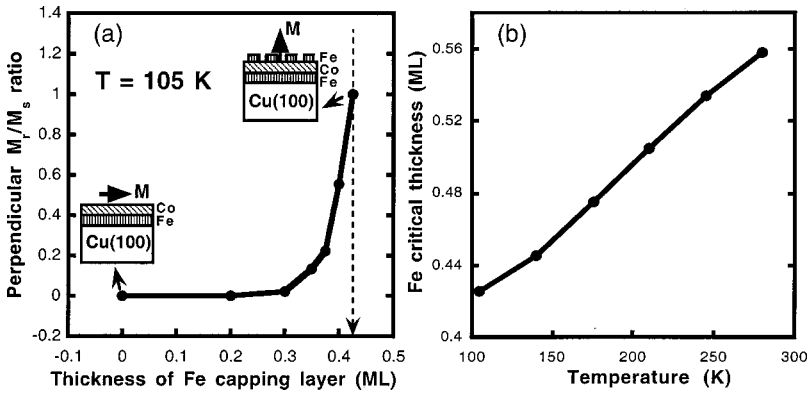

FIG. 4. (a) Reverse spin reorientation in 1.2-ML Co/1.2-ML Fe bilayer on Cu(100) induced by Fe capping layer. At 105 K, 0.43 ML of Fe (indicated by the dashed arrow) is required to complete the inplane to perpendicular spin reorientation. (b) The Fe critical thickness of the reverse spin reorientation as a function of temperature.

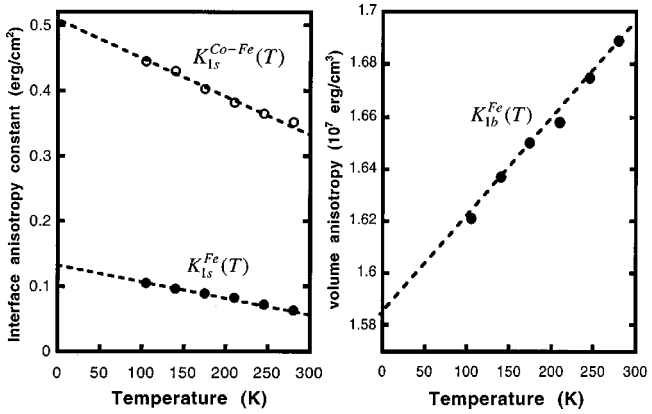

FIG. 5. Temperature-dependent anisotropy constants for the Co capped Fe/Cu(100) system. All anisotropy constants display a linear dependence on the temperature. The dashed lines are present to guide the eye.

left and right boundaries of the transition regime define the onset and completion of the SRT of Fe films, respectively. To make the phase diagram more complete, we have included the Curie temperatures (filled squares) of Fe films that are thinner than four atomic layers. These values are in good agreement with Ref. 10.

From the obtained phase diagram, it is immediately clear that the critical temperature of SRT is slightly lower than the Curie temperature in the Fe/Cu(100) system. The system would first undergo an SRT before becoming paramagnetic, when increasing thickness or temperature. Since the marked region, in which the stripeless phase was observed in Ref. 1, is closer to the SRT temperature than to the Curie temperature, we believe that the melting of the stripe phase is caused by the onset of an SRT rather than by paramagnetism. This is not surprising, since the system no longer has enough perpendicular anisotropy to sustain the up-down stripe domains when approaching the SRT. A similar breakdown of perpendicular domains has been observed in the low temperature grown Fe/Cu(100) system.[14]

It is interesting that a temperature-driven SRT has never been reported for the RT grown Fe films, although the observation is difficult in practice because the SRT temperature is very close to the structural-relaxation temperature ($\sim$310 K).[15]

The magnetic phase diagram can be used to calculate the temperature-dependent anisotropy constants of the Fe films. Recently, Millev and co-workers were able to deduce both first- (K_{1s}) and second-order (K_{2s}) surface anisotropy constants with[16] and without[17] an external field. In principle, since we have the data of the first and second critical thickness of SRT at various temperatures (Fig. 3), we should be able to obtain the values of temperature-dependent K_{1s} and K_{2s} following the same approach. However, the calculation cannot be made without values for the first- (K_{1b}) and second-order (K_{2b}) bulk anisotropy constants of fcc Fe, which are lacking due to the fact that fcc Fe does not exist below 1150 K in bulk. It is not proper to use the bulk anisotropy constants of bcc Fe in this case. This is not only because bcc Fe has a different crystal structure, but also because the Fe/Cu(100) films have a greatly distorted fcc structure. This should lead to considerably larger bulk anisotropy constants than those of undistorted bcc Fe.

For the reasons described above, we decide to concentrate only on obtaining first-order anisotropy constants for both surface and bulk. This, in fact, is nontrivial since the spin phase diagram alone does not provide enough information to deduce both the surface and bulk anisotropy constants of Fe/Cu(100) films. We, therefore, designed an experiment by using Fe capping layers to introduce a reversed SRT in a Co/Fe bilayer on Cu(100), as shown in Fig. 4. In the reversed SRT experiment, a 1.2 ML Co/1.2 ML Fe bilayer structure was first grown on top of Cu(100) at room temperature. This bilayer structure has an in-plane easy magnetization axis. Additional Fe atoms were then deposited on the Co/Fe bilayer at 105 K until the film was fully magnetized in the perpendicular direction [marked by the arrow with dashed line in Fig. 4(a)]. The amount of Fe needed to complete this reversed SRT is denoted as $d_{c,2}^{\mathrm{Co/Fe}}$, the temperature dependence of which is shown in Fig. 4(b). Based on the argument made in Ref. 16, the first-order crystalline anisotropy (including both surface and bulk) cancels out with shape anisotropy at the thickness, where SRT has been completed, i.e., $K_1 = K_{1b} + 2K_{1s}/d_{c,2} = 2\pi M^2$. We have determined the temperature-dependent values of $d_{c,2}$ for three SRT's, namely, the SRT of Fe/Cu(100) ($d_{c,2}^{\mathrm{Fe}}$), the Co-induced SRT of Fe/Cu(100) ($d_{c,2}^{\mathrm{Co}}$), and the Fe-induced SRT of Co/Fe bilayer on Cu(100) ($d_{c,2}^{\mathrm{Co/Fe}}$). For the SRT of Fe/Cu(100), we have

$$K_{1b}^{\mathrm{Fe}}(T) + \frac{2K_{1s}^{\mathrm{Fe}}(T)}{d_{c,2}^{\mathrm{Fe}}(T)} = 2\pi M_{\mathrm{Fe}}(T)^2. \tag{1}$$

TABLE I. Temperature-dependent parameters in Eqs. (1), (2), and (3). Note that values of $K_{1b}^{\mathrm{Co}}(T)$ and $K_{1s}^{\mathrm{Co}}(T)$ are taken from Ref. 17.

Temperature (K)	$d_{c,2}^{\mathrm{Fe}}(T)$ (10^{-8} cm)	$d_{c,2}^{\mathrm{Co}}(T)$ (10^{-8} cm)	$d_{c,2}^{\mathrm{Co/Fe}}$ (10^{-8} cm)	$\varphi(T)$	$\varepsilon(T)$	$K_{1b}^{\mathrm{Co}}(T)$ (10^6 erg/cm^3)	$K_{1s}^{\mathrm{Co}}(T)$ (erg/cm^2)
105	9.31	0.69	0.77	0.41	0.43	−9.78	−0.478
140	9.20	0.67	0.80	0.39	0.44	−9.97	−0.437
175	9.11	0.64	0.86	0.38	0.48	−10.16	−0.399
210	8.80	0.62	0.91	0.36	0.51	−10.34	−0.360
245	8.44	0.58	0.96	0.34	0.53	−10.53	−0.320
280	8.05	0.55	1.00	0.32	0.56	−10.72	−0.281

For the Co-induced SRT of Fe/Cu(100), we have

$$\left(\frac{K_{1b}^{\mathrm{Fe}}(T)\times d_{\mathrm{Fe}}+K_{1b}^{\mathrm{Co}}(T)\times d_{c,2}^{\mathrm{Co}}(T)}{d_{\mathrm{Fe}}+d_{c,2}^{\mathrm{Co}}(T)}\right)+\frac{\{[2-\varphi(T)]K_{1s}^{\mathrm{Fe}}(T)+\varphi(T)[K_{1s}^{\mathrm{Co}}(T)+K_{1s}^{\mathrm{Co\text{-}Fe}}(T)]\}}{[d_{\mathrm{Fe}}+d_{c,2}^{\mathrm{Co}}(T)]}=2\pi\left(\frac{M_{\mathrm{Fe}}(T)\times d_{\mathrm{Fe}}+M_{\mathrm{Co}}(T)\times d_{c,2}^{\mathrm{Co}}(T)}{d_{\mathrm{Fe}}+d_{c,2}^{\mathrm{Co}}(T)}\right)^2, \tag{2}$$

where d_{Fe} is the thickness of the Fe base film, and $\varphi(T)$ is the coverage of the Co capping layer at the critical thickness of the SRT, which is the same as $d_{c,2}^{\mathrm{Co}}(T)$ when it is expressed in units of monolayers.

For the Fe induced SRT of Co/Fe bilayer on Cu(100), we have

$$\frac{K_{1b}^{\mathrm{Fe}}(T)\times[d_{\mathrm{Fe}}^{*}+d_{c,\mathrm{Fe}}(T)]+K_{1b}^{\mathrm{Co}}(T)\times d_{\mathrm{Co}}^{*}}{d_{\mathrm{Fe}}^{*}+d_{c,2}^{\mathrm{Co/Fe}}(T)+d_{\mathrm{Co}}^{*}}+\frac{[1+\varepsilon(T)][K_{1s}^{\mathrm{Fe}}(T)+K_{1s}^{\mathrm{Co\text{-}Fe}}(T)]+[1-\varepsilon(T)]K_{1s}^{\mathrm{Co}}(T)}{d_{\mathrm{Fe}}^{*}+d_{c,2}^{\mathrm{Co/Fe}}(T)+d_{\mathrm{Co}}^{*}}=2\pi\left(\frac{M_{\mathrm{Fe}}(T)\times[d_{\mathrm{Fe}}^{*}+d_{c,2}^{\mathrm{Co/Fe}}(T)]+M_{\mathrm{Co}}(T)\times d_{\mathrm{Co}}^{*}}{d_{\mathrm{Fe}}^{*}+d_{c,2}^{\mathrm{Co/Fe}}(T)+d_{\mathrm{Co}}^{*}}\right)^2, \tag{3}$$

where d_{Fe}^{*} and d_{Co}^{*} are the thickness of Fe and Co in the Fe/Co bilayer, respectively, and $\varepsilon(T)$ is equal to $d_{c,2}^{\mathrm{Co/Fe}}$ in units of monolayers.

The first-order bulk $[K_{1b}^{\mathrm{Co}}(T)]$ and surface $[K_{1s}^{\mathrm{Co}}(T)]$ anisotropy constants of fcc Co(100) have been determined by Kowalewski, Schneider, and Heinrich using ferromagnetic resonance measurements on ultrathin films of Co/Cu(100).[18] Although anisotropy constants were measured at only two temperatures (77 and 295 K), it is reasonable to assume a linear temperature dependence and get anisotropy constants at other temperatures. By further taking bulk values of the magnetization of Fe$[M_{\mathrm{Fe}}(T)]$ and Co$[M_{\mathrm{Co}}(T)]$, we have three unknowns, i.e., $K_{1b}^{\mathrm{Fe}}(T)$, $K_{1s}^{\mathrm{Fe}}(T)$, and $K_{1s}^{\mathrm{Co\text{-}Fe}}(T)$, left in Eqs. (1), (2), and (3). For the convenience of readers, the known values of $d_{c,2}^{\mathrm{Fe}}(T)$, $d_{c,2}^{\mathrm{Co}}(T)$ (at $d_{\mathrm{Fe}}=0$), $d_{c,2}^{\mathrm{Co/Fe}}$, $K_{1b}^{\mathrm{Co}}(T)$, $K_{1s}^{\mathrm{Co}}(T)$, $\varphi(T)$, and $\varepsilon(T)$ at various temperatures are summarized in Table I. After some calculations, we have obtained values of $K_{1b}^{\mathrm{Fe}}(T)$, $K_{1s}^{\mathrm{Fe}}(T)$, and $K_{1s}^{\mathrm{Co\text{-}Fe}}(T)$ as a function of temperature, as shown in Fig. 5. From Fig. 5 it is obvious that all these contributions to the anisotropy are positive (favoring perpendicular magnetization) and have a linear temperature dependence. The values of $K_{1s}^{\mathrm{Fe}}(T)$ and $K_{1s}^{\mathrm{Co\text{-}Fe}}(T)$, as expected, decrease with increasing temperature. It is somewhat surprising that $K_{1b}^{\mathrm{Fe}}(T)$ increases with increasing temperature. In light of the possibility that $K_{1b}^{\mathrm{Fe}}(T)$ most likely originates from strain-induced anisotropy, the increase of $K_{1b}^{\mathrm{Fe}}(T)$ might be caused by an increase in film strain due to the different thermal-expansion coefficients of fct Fe and fcc Cu. Similar behavior was also observed for Co ultrathin films on Cu(100).[18]

In summary, we have demonstrated that magnetic capping layers can be used to generate a magnetic phase diagram for metastable magnetic Fe/Cu(100) ultrathin films. The magnetic phase diagram uncovers important information about the phase transitions of the Fe/Cu(100) system. In addition, we have shown that the anisotropy constants of Fe films display a linear temperature dependence. We believe that this method can be generalized to other metastable magnetic thin-film systems.

The authors would like to thank R. Vollmer and J. Kirschner for insightful discussion. This research was sponsored by the U.S. Department of Energy under Contract No. DE-AC05-00OR22725 with the Oak Ridge National Laboratory, managed by UT-Battelle, LLC, and the U.S. National Science Foundation under Contract No. DMR-9801830.

*Corresponding author.

[1] A. Vaterlaus, C. Stamm, U. Maier, M. G. Pini, P. Politi, and D. Pescia, Phys. Rev. Lett. **84**, 2247 (2000).
[2] K. L. Man, M. S. Altman, and H. Poppa, Surf. Sci. (to be published).
[3] Ar. Abanov, V. Kalatsky, and V. L. Pokrovsky, Phys. Rev. B **51**, 1023 (1995).
[4] J. Thomassen, F. May, B. Feldmann, M. Wuttig, and H. Ibach, Phys. Rev. Lett. **69**, 3831 (1992).
[5] Dongqi Li, M. Freitag, J. Pearson, Z. Q. Qiu, and S. D. Bader, Phys. Rev. Lett. **72**, 3112 (1994).
[6] M. Straub, R. Vollmer, and J. Kirschner, Phys. Rev. Lett. **77**, 743 (1996).
[7] J. Giergiel, J. Kirschner, J. Landgraf, J. Shen, and J. Woltersdorf, Surf. Sci. **310**, 1 (1994).
[8] K. Kalki, D. D. Chambliss, K. E. Johnson, R. J. Wilson, and S. Chiang, Phys. Rev. B **48**, 18 344 (1993).
[9] S. Müller, P. Bayer, C. Reischl, K. Heinz, B. Feldmann, H. Zillgen, and M. Wuttig, Phys. Rev. Lett. **74**, 765 (1995).
[10] A. Biedermann, M. Schmid, and P. Varga, Phys. Rev. Lett. **86**, 464 (2001).
[11] J. Lee, G. Lauhoff, and J. A. C. Bland, Phys. Rev. B **56**, R5728 (1997).
[12] M. A. Torija, J. P. Pierce, and J. Shen, Phys. Rev. B **63**, 092404 (2001).
[13] J. Shen, A. K. Swan, and J. F. Wendelken, Appl. Phys. Lett. **75**, 2987 (1999).
[14] R. Allenspach and A. Bischof, Phys. Rev. Lett. **69**, 3385 (1992).
[15] M. Zharnikov, A. Dittschar, W. Kuch, C. M. Schneider, and J. Kirschner, Phys. Rev. Lett. **76**, 4620 (1996).
[16] Y. T. Millev and J. Kirschner, Phys. Rev. B **54**, 4137 (1996); H. P. Oepen, M. Speckmann, Y. Millev, and J. Kirschner, *ibid.* **55**, 2752 (1997).
[17] Y. T. Millev, H. P. Oepen, and J. Kirschner, Phys. Rev. B **57**, 5837 (1998).
[18] M. Kowalewski, C. M. Schneider, and B. Heinrich, Phys. Rev. B **47**, 8748 (1993).